Available online at www.sciencedirect.com
ScienceDirect
Electrochimica Acta 53 (2008) 3508–3513
ELECTROCHIMICA Acta
www.elsevier.com/locate/electacta

The polarization behavior of the anode in a microbial fuel cell

Aswin K. Manohar [a], Orianna Bretschger [a,b], Kenneth H. Nealson [b], Florian Mansfeld [a,*,1]

[a] *Corrosion and Environmental Effects Laboratory (CEEL), The Mork Family Department of Chemical Engineering and Materials Science, University of Southern California, Los Angeles, CA 90089-0241, USA*
[b] *Department of Earth Sciences, University of Southern California, Los Angeles, CA 90089-0241, USA*

Received 8 August 2007; received in revised form 1 December 2007; accepted 1 December 2007
Available online 24 January 2008

Abstract

Microbial fuel cell (MFC) systems are unique electrochemical devices that employ the catalytic action of bacteria to drive the oxidation of organic compounds. These systems have been suggested as renewable energy sources for small remote devices; however, questions remain about how MFCs can be efficiently optimized for this purpose. Several electrochemical techniques have been employed in this study to elucidate the limiting factors in power production by MFCs. Impedance spectra were collected for the anode and cathode at their open-circuit potential (OCP) before and after all other electrochemical tests. Cell voltage–current curves were obtained using a potential sweep technique and used to determine the maximum power available from the system. Potentiodynamic polarization in two different potential regions was used to determine the exchange current for the reaction occurring at the anode at its OCP and to explore the polarization behavior of the anode and the cathode in a wide potential range. Cyclic voltammetry was used to evaluate the redox activity of the anode. These techniques used in combination showed that the microorganism *Shewanella oneidensis* MR-1 is solely responsible for the observed decrease of the OCP of the anode, the increased rate of oxidation of lactate, the larger cell voltage and the increased maximum power output of the MFC.

Keywords: Microbial fuel cell; Electrochemistry; Electrochemical impedance spectroscopy; Cyclic voltammetry; Polarization curves; Electrode kinetics

1. Introduction

A survey of the ever-increasing literature dealing with microbial fuel cell (MFC) systems suggests that a select number of advanced electrochemical techniques are routinely utilized to characterize the properties and performance of MFCs. Several authors have used cyclic voltammetry [1–7] (CV) and chronoamperometry [8] to characterize MFC systems; however, there are very few papers in which electrochemical impedance spectroscopy (EIS) and anodic and cathodic polarization curves have been used to determine system parameters and limitations. Logan and co-workers [9] and He et al. [10] used EIS to determine the internal resistance of a MFC, however they did not employ further analysis to their EIS spectra to determine redox reaction rates or surface area characteristics of their electrodes.

In a previous investigation [11], MFC performance was investigated using potential sweep techniques, EIS, CV and potentiodynamic polarization curves to characterize the electrochemical properties of the anode and cathode for different experimental conditions over a 4-week period. In the present study, these electrochemical techniques were used again to evaluate the polarization behavior of the anode in more detail using anolytes containing buffer, buffer and lactate, or buffer, lactate and the bacteria *Shewanella oneidensis* MR-1.

2. Materials and methods

2.1. Microbial fuel cell system

Electrochemical experiments were conducted using dual compartment MFC systems with each compartment holding a volume of 25 mL [11,12]. The electrodes consisted of a graphite felt anode and a platinum coated graphite cathode. A proton exchange membrane (Nafion 424, DuPont) separated the anode and cathode compartments. Each electrode had an apparent sur-

* Corresponding author. Tel.: +1 213 740 3016; fax: +1 213 740 7797.
E-mail address: mansfeld@usc.edu (F. Mansfeld).
[1] ISE Member.

0013-4686/$ – see front matter © 2007 Elsevier Ltd. All rights reserved.
doi:10.1016/j.electacta.2007.12.002

face area of 20 cm^2 and was connected to Pt-wire leads by a conductive carbon epoxy (EPOX, Electrolytica).

The assembled MFC was autoclaved at 121 °C for 15 min prior to the addition of any liquid media. Sterile Ag/AgCl reference electrodes were inserted into both the anode and cathode compartments after autoclaving. Anaerobic conditions were maintained in the MFC anode by continuously passing filtered nitrogen gas through the compartment at a rate of 20 mL/min. Aerobic conditions were maintained in the cathode compartment by continuously passing air at a rate of 40 mL/min.

Electrochemical measurements were performed under three different anode conditions: (1) buffer alone as anolyte, (2) buffer and lactate (20 mM) and (3) buffer, lactate (20 mM) and *Shewanella oneidensis* MR-1 in the anode compartment. The buffer solution contained 50 mM PIPES ($C_8H_{18}N_2O_6S_2$) and 7.5 mM NaOH (pH 7.0). The same buffer solution was used in the anode and the cathode compartments. The same cell was used for the three sets of experiments. Prior to each type of electrochemical measurement, the MFC was allowed to remain at the open-circuit cell voltage V_0 for several hours, such that a stable open-circuit cell potential could be observed for the anode (OCP^a) and the cathode (OCP^c) electrodes before measurements were taken.

2.2. Bacterial growth conditions

2.2.1. Shewanella oneidensis

MR-1 was grown in a PIPES-buffered minimal media (pH 7.0) containing 18 mM lactate as the sole electron donor, 50 mM PIPES, 7.5 mM NaOH, 28 mM NH_4Cl, 1.3 mM KCl, 4.3 mM $NaH_2PO_4{\cdot}H_2O$ and 10 mL/L each of vitamin, amino acid and trace mineral stock solutions. Batch cultures were grown at 30 °C and agitated at a rate of 140 rpm until the late stationary phase was achieved. The cells were then harvested and injected into the MFC such that an optical density at 600 nm (OD_{600}) of 0.4 was achieved in the anode compartment using PIPES buffer as the diluting medium [12].

2.3. Electrochemical techniques

A Gamry PCI4/300 potentiostat was used for all electrochemical measurements. Gamry EIS300 software was used for recording of impedance spectra, DC105 software was used for collecting potentiodynamic polarization curves and PHE200 software was used for carrying out the CV experiments.

2.3.1. Electrochemical impedance spectroscopy (EIS)

EIS was performed at the start and at the end of a set of experiments for both the anode and the cathode using a Ag/AgCl reference electrode. Anode impedance spectra were recorded using the anode as the working electrode and the cathode as the counter electrode. Cathode impedance spectra were recorded using the cathode as the working and the anode as the counter electrode. All EIS evaluations were conducted at the OCP in a frequency range of 100 kHz–5 mHz. The amplitude of the applied ac signal was 10 mV. The EIS data for different anolytes in the anode compartment and for the cathode are plotted in the form of Bode plots in which the logarithm of the modulus of the impedance $|Z|$ and the phase angle Φ are plotted vs. the logarithm of the frequency f of the applied ac signal.

2.3.2. Potential sweeps

Potential sweep experiments were carried out at a scan rate of 0.1 mV/s from the open-circuit cell voltage V_0, where $I = 0$, to the short-circuit cell voltage $V_{sc} = 0$, where $I = I_{max}$. From the V–I curves power (P)–V curves were calculated. The P–V curves were used to determine the cell voltage V_{max} at which the maximum power output was produced.

2.3.3. Cyclic voltammetry (CV)

CV was performed for the anode in the three different test solutions using a potential range of −700 mV to +750 mV (vs. Ag/AgCl) at a scan rate of 25 mV/s.

2.3.4. Potentiodynamic polarization

Polarization curves were recorded for the anode and cathode. Three types of polarization curves were obtained: (1) anodic polarization curve for the anode; (2) cathodic polarization curve for the anode; and (3) cathodic polarization curve for the cathode. The anodic polarization curve for the anode was recorded in the potential region from OCP^a −30 mV to +1 V (vs. Ag/AgCl). The cathodic polarization curves for the anode and the cathode were measured between OCP^c + 30 mV and −1 V (vs. Ag/AgCl). Polarization experiments were also performed for the anode in the vicinity of OCP^a.

2.4. Test sequence

The MFC was assembled with the anode compartment containing buffer solution only. The cycle of electrochemical experiments was started by collecting an impedance spectrum at the OCP for the anode and the cathode. This was followed by the potential sweep test and another EIS test. Then CV was carried out for the anode followed by the polarization experiments for the anode and the cathode. The same sequence of experiments was repeated after the anolyte was replaced with a solution containing buffer and lactate, and then again with the anolyte containing buffer, lactate and MR-1. The same MFC assembly, i.e. the same electrodes and membrane, was used for all tests.

3. Results and discussion

3.1. EIS

EIS data were collected before and after the completion of the various polarization tests. The fit parameters for these data are discussed below and are listed in Tables 1 and 2. The spectra for the anode and cathode obtained prior to any polarization experiments were nearly identical to those collected upon completion of the test series for every anolyte condition (data not shown). The similarity of EIS data collected before and after polarization indicates that the electrode properties were not affected

Table 1
Open circuit potential (OCP), polarization resistance (R_p) and capacitance (C) of the anode before and after tests with different anolytes

	Buffer only		Buffer and lactate		Buffer, lactate and MR-1	
	Before tests	After tests	Before tests	After tests	Before tests	After tests
OCP (V)	0.195	0.190	0.220	0.230	−0.525	−0.497
R_p (kΩ)	429.1	356.0	292.1	290.0	34.6	32.3
C (mF)	2.11	2.20	3.88	3.80	4.21	4.20

Table 2
Open circuit potential (OCP), polarization resistance (R_p) and capacitance (C) of the cathode before and after tests with different anolytes

	Buffer only		Buffer and lactate		Buffer, lactate and MR-1	
	Before tests	After tests	Before tests	After tests	Before tests	After tests
OCP (V)	0.350	0.324	0.340	0.330	0.348	0.290
R_p (kΩ)	9.83	11.0	10.05	9.90	16.41	16.04
C (mF)	98.2	96.0	97.9	98.0	67.7	68.1

by drawing a current. Given the similarity of spectra for measurements collected before and after each polarization test, only those data obtained before the completion of each test are shown for the anode and cathode in Fig. 1a and b, respectively. The spectra in Fig. 1a show that the polarization resistance (R_p^a) of the anode decreased slightly upon the addition of lactate and

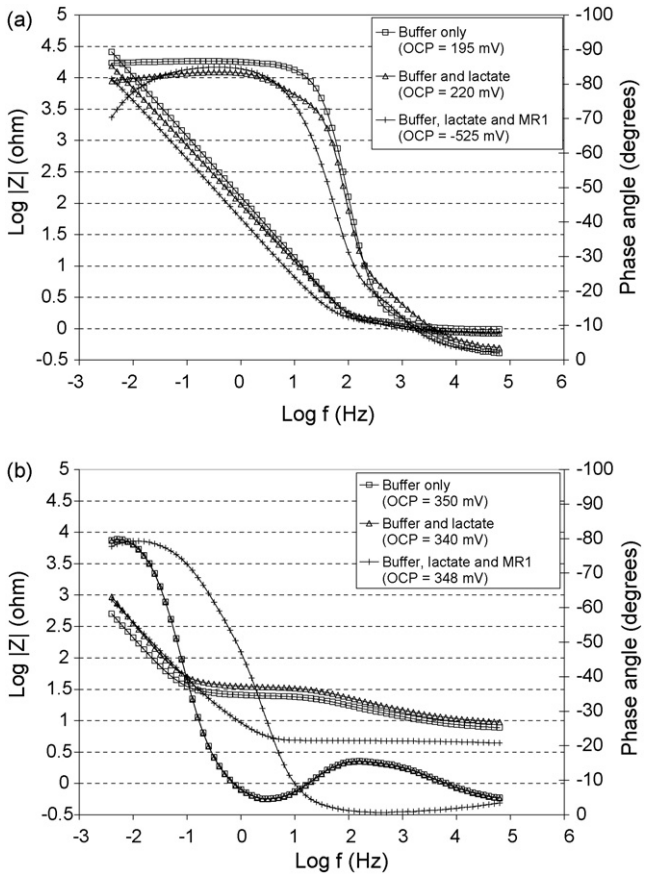

Fig. 1. Impedance spectra for tests with three different anolytes for the (a) anode and (b) cathode. The spectra were obtained throughout the test series before another test was carried out.

that the addition of MR-1 to the anode compartment produced a significant change in the impedance response of the anode. The low-frequency dependence of the phase angle indicates that the polarization resistance of the anode (R_p^a) had decreased significantly.

The polarization resistance of the cathode (R_p^c) is a factor of 30 lower than (R_p^a) for the anolyte conditions without MR-1; however, (R_p^c) and (R_p^a) are within the same order of magnitude when MR-1 are present in the anolyte (Fig. 1). The low-frequency dependence of the phase angle indicates that the (R_p^c) remains low and relatively constant under all anolyte conditions. The capacitance of the cathode is much larger than that of the anode due to the large active surface area of the Pt-plated cathode (Tables 1 and 2).

The impedance spectra in Fig. 1 follow a one-time-constant (OTC) model where the solution resistance R_s is in series with a parallel combination of the capacitance of the electrode C and the polarization resistance R_p which is inversely proportional to the exchange current I_0 for the redox reaction occurring at the electrode [13]. The impedance modulus $|Z|$ for the OTC model is given by [14]:

$$|Z| = R_s + R_p/(1 + (j\omega C R_p)^{\alpha}), \quad (1)$$

where $\omega = 2\pi f$ and $0 \leq \alpha \leq 1$.

The spectra were analyzed using the ANALEIS software developed by Mansfeld and co-workers [15–17]. Fig. 2 gives a comparison of the experimental data for the anode and the cathode before the polarization tests in the presence of MR-1 (Fig. 1) and the fitted data. Excellent agreement between the two data sets is observed. A drastic decrease of the OCP is accompanied by a decrease of R_p by about factor of 10 for the anode in the presence of MR-1. The capacitance seems to increase slightly in the presence of lactate and again when MR-1 is present in the anode (Table 1). No significant changes in the impedance parameters seem to occur for the cathode in the three test series (Table 2).

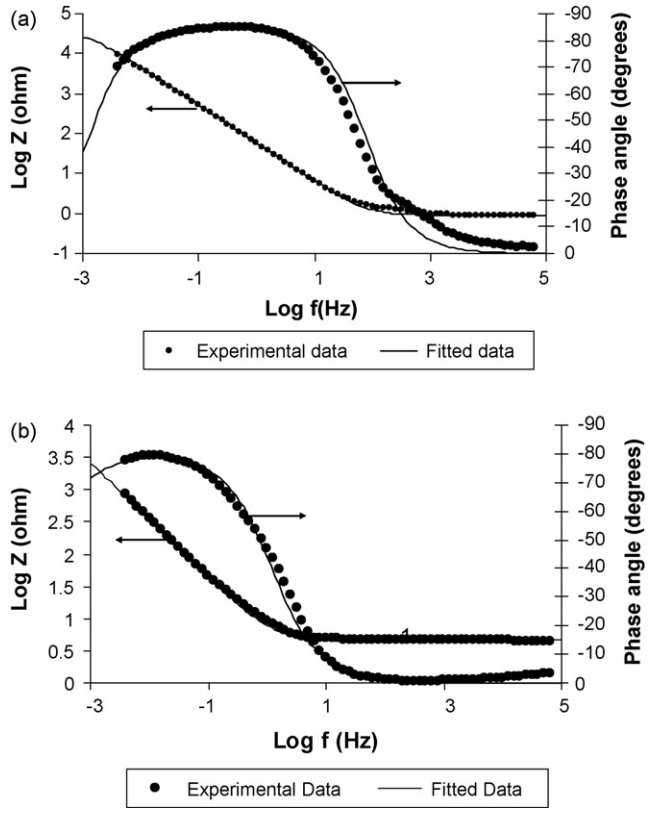

Fig. 2. Comparison of experimental and fitted impedance spectra for the (a) anode with buffer, lactate and MR-1 as the anolyte, and (b) cathode with buffer only (Fit parameters for the anode: $C = 4.21 \times 10^{-3}$ F, $R_p = 3.46 \times 10^4\ \Omega$, $R_s = 0.92\ \Omega$; Fit parameters for the cathode: $C = 6.77 \times 10^{-2}$ F, $R_p = 1.64 \times 10^4\ \Omega$, $R_s = 4.7\ \Omega$).

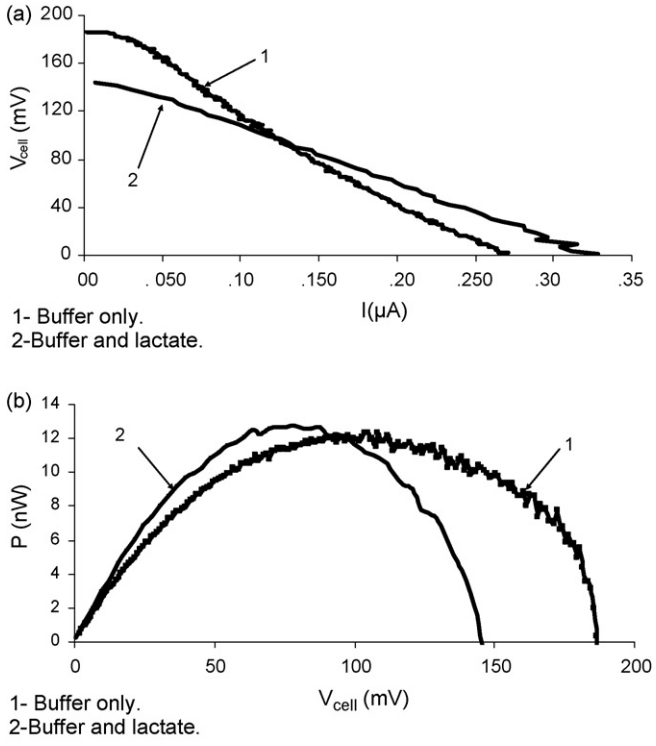

Fig. 3. (a) V_{cell}–I and P–V_{cell} (b) curves for tests with buffer only and with buffer and lactate as anolyte.

3.2. Potential sweeps

The V–I and P–V curves for tests in buffer only and for buffer and lactate in the anode compartment are shown in Fig. 3a and b, respectively. The cell voltage decreased somewhat in the presence of lactate, but the maximum current (I_{max}) was slightly higher (Fig. 3a). These differences are reflected in the P–V curves in Fig. 3b. The V–I and P–V curves obtained in the presence of MR-1 (Fig. 4a and b, respectively) show that the cell voltage V_0 increased from 180 mV (buffer only and buffer and lactate anolytes) to about 820 mV. I_{max} also increased in the presence of MR-1 from 0.33 μA to 160 μA and the maximum power output increased from 0.012 μW to 20 μW. This power output was found to be nearly constant over a cell voltage range between 200 mV and 600 mV.

3.3. CV

The cyclic voltammograms generated for the anolyte containing buffer only (Fig. 5a) showed no significant redox peaks. However, a reduction peak at about −250 mV and an oxidation peak at about 200 mV were observed when the test was performed with buffer and lactate as the anolyte. The current flow in the voltammogram obtained when the anolyte contained buffer, lactate and MR-1 (Fig. 5b) was significantly higher in all potential regions than the current for the voltammograms obtained from the other two anolytes. A reduction peak was observed at about −500 mV, while the oxidation peak was observed to be at the same potential of about 200 mV.

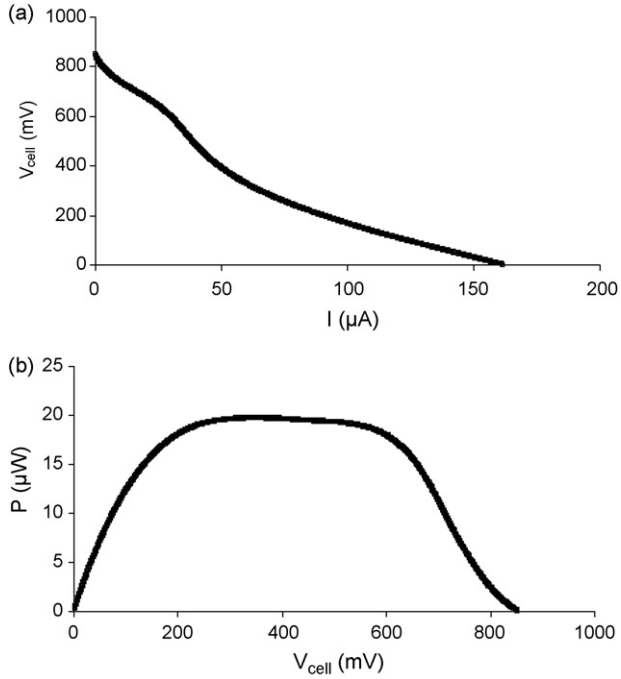

Fig. 4. (a) V_{cell}–I and (b) P–V_{cell} curves for test with buffer, lactate and MR-1 as anolyte.

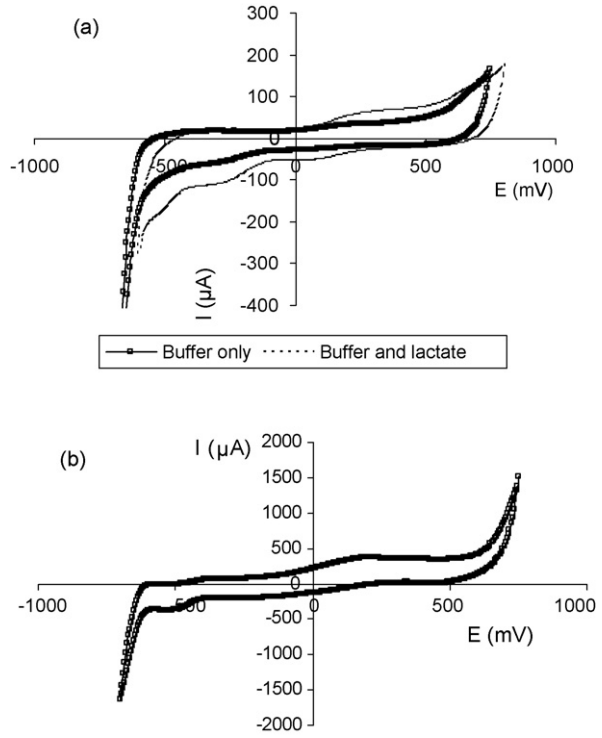

Fig. 5. Cyclic voltammograms for the anode for tests with (a) buffer only and with buffer and lactate and (b) for test with buffer, lactate and MR-1.

3.4. Potentiodynamic polarization

Fig. 6 shows the polarization curve for the anode in buffer, lactate and MR-1 as the electrolyte in the potential region $-20\,\text{mV} \leq \text{OCP}^a \leq 40\,\text{mV}$. Polarization curves were analyzed with the program POLFIT [18], in which the experimental data are fit to the Butler–Volmer Eq.:

$$I = I_0\{\exp(E - E_0/b_a) - \exp(E_0 - E/b_c)\} \quad (2)$$

From this analysis, the exchange current (I_0), the anodic Tafel slope (b_a) and the cathodic Tafel slope (b_c) can be determined in the pre-Tafel region [18]. R_p and I_0 are related by $I_0 = B/R_p$, where $B = b_a b_c/2.303(b_a + b_c)$. The results of the analysis using POLFIT are given in Table 3. The presence of MR-1 in the anolyte increased the value of I_0 by a factor of about 10, whereas I_0 had similar values in anolytes not containing MR-1.

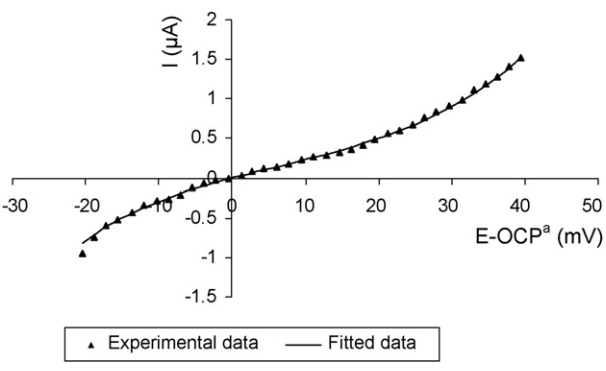

Fig. 6. Polarization curve in the vicinity of OCP[a] for the anode with buffer, lactate and MR-1 as anolyte.

Table 3
Results of analysis of polarization curve for the anode

Anolyte	I_0 (μA)	b_a (mV)	b_c (mV)
Buffer only	0.024	75	44
Buffer and lactate	0.021	106	25
Buffer, lactate and MR-1	0.185	43	30

The results of the polarization experiments performed in a larger potential range shown in Fig. 7 indicate that the OCP[a] became much more negative after the addition of MR-1 to the anode compartment as indicated previously in the results obtained in the recording of EIS data (Fig. 1). The polarization curves for tests with the anolyte containing buffer only and buffer and lactate did not show much difference, however the oxidation currents that were observed when the anode compartment contained MR-1 were much higher compared to the other conditions.

The cathodic polarization curve for the cathode shows charge-transfer control at low overpotentials followed by two regions of mass transport control (Fig. 7). The cathodic polarization curve for the cathode intersects the anodic polarization curve for the anode with anolyte containing MR-1 at about 100 μA, as compared to an intersection at <1 μA for the other two conditions (Fig. 7). From these data it is apparent that 100 μA is the maximum current that can be drawn from this MFC under these specific operating conditions. The maximum current shown in Fig. 4a is approximately 160 μA. The slight discrepancy between this value and the value estimated in Fig. 7 could be explained by the time sequence of these experiments. The polarization curve shown in Fig. 4a was obtained immediately after MR-1 was inoculated into the fuel cell, fed lactate, and the OCP stabilized. The potentiodynamic polarization experiments were performed after a series of other tests and therefore the viability of the bacteria may have changed, thereby affecting the overall performance of the cell.

4. Summary and conclusions

The impedance spectra, the cyclic voltammograms and the polarization curves for the anode have all demonstrated that addition of MR-1 to the MFC anolyte greatly increases the rate of the lactate oxidation reaction that occurs at OCP[a]. The impedance spectra showed that the electrochemical properties of the anode and the cathode did not change very much despite extensive polarization. An analysis of the polarization curves obtained in the vicinity of OCP[a] indicated a large increase of I_o upon the addition of MR-1 to the MFC system (Table 3).

The *V–I* and the *P–V* curves demonstrate that the addition of MR-1 to the anolyte containing lactate greatly increased the cell voltage and the power output of the MFC. The very large changes of the cell voltage and cell current can be seen best in the V_{cell}—log *I* curves shown in Fig. 8 for the three different anolytes. While in the absence of MR-1 the maximum power was about 0.12 μW (Fig. 3), it was close to 20 μW in the presence

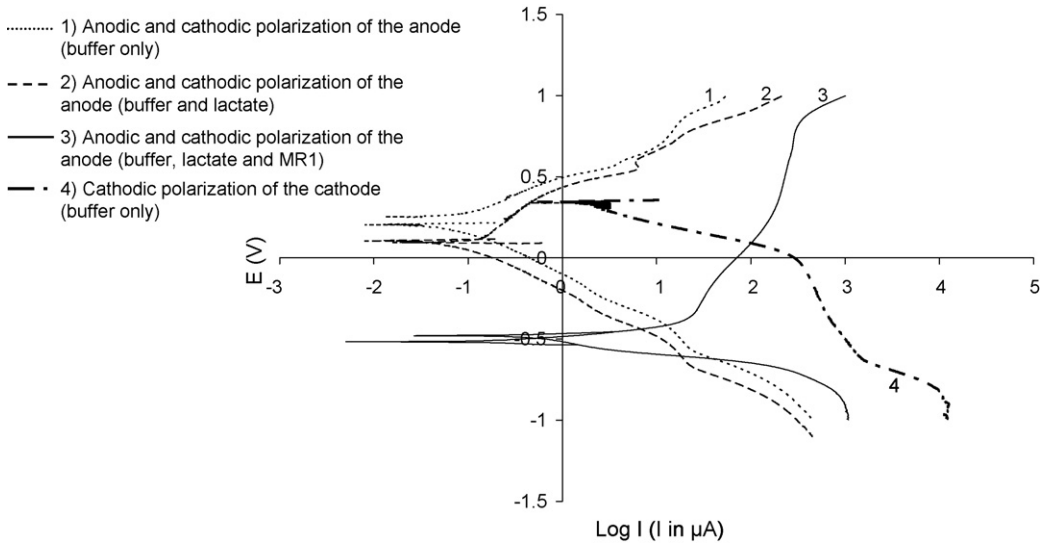

Fig. 7. Polarization curves for the anode in three different anolytes and for the cathode in buffer solution.

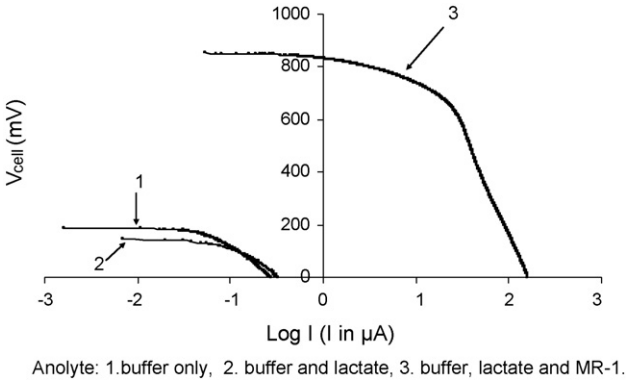

Fig. 8. V_{cell}–log I curves for three different test conditions.

of MR-1, where a constant power output was found in a cell voltage range between 200 mV and 600 mV (Fig. 4).

Acknowledgements

This project is supported by the AFOSR MURI program, Award No. FA9550-06-1-0292, Maj. Jennifer Gresham, contract monitor.

References

[1] K. Rabaey, N. Boon, S.D. Siciliano, M. Verhaege, W. Verstraete, Appl. Environ. Microbiol. 70 (2004) 5373.
[2] F. Zhao, F. Harnisch, U. Schroder, F. Scholz, P. Bogdanoff, I. Herrmann, Environ. Sci. Technol. 40 (2006) 5193.
[3] D.H. Park, J.G. Zeikus, Appl. Environ. Microbiol. 66 (2000) 1292.
[4] D.H. Park, G.J. Zeikus, Biotechnol. Bioeng. 81 (2003) 348.
[5] E.J. Cho, A.D. Ellington, Bioelectrochemistry 70 (2007) 165.
[6] D. Prasad, S. Arun, M. Murugesan, S. Padmanaban, R.S. Satyanarayanan, S. Berchmans, V. Yegnaraman, Biosens. Bioelectron. 22 (2007) 2604.
[7] H.J. Kim, H.S. Park, M.S. Hyun, I.S. Chang, M. Kim, B.H. Kim, Enzyme Microb. Technol. 30 (2002) 145.
[8] U. Schröder, J. Nießen, F. Scholz, Angew. Chem. Int. Ed. 42 (2003) 2880.
[9] B. Min, S. Cheng, B.E. Logan, Water Res. 39 (2005) 1675.
[10] Z. He, N. Wagner, S.D. Minteer, L.T. Angenent, Environ. Sci. Technol. 40 (2006) 5212.
[11] A.K. Manohar, O. Bretschger, K.H. Nealson, F. Mansfeld, An evaluation of the performance of a microbial fuel cell using different electrochemical techniques, Electrochim. Acta, in press.
[12] O. Bretschger, A. Obraztsova, C.A. Sturm, I.-S. Chang, Y.A. Gorby, S.B. Reed, D.E. Culley, C.L. Reardon, S. Barua, M.F. Romine, J. Zhou, A.S. Beliaev, R. Bouhenni, D. Saffarini, F. Mansfeld, B.-H. Kim, J.K. Fredrickson, K.H. Nealson, Appl. Environ. Microbiol. 73 (2007) 7003.
[13] F. Mansfeld, in: M.G. Fontana, R.W. Staehle (Eds.), Advances in Corrosion Science and Technology, Plenum Press, 1976, p. 163.
[14] F. Mansfeld, W.J. Lorenz, in: R. Varma, J.R. Selman (Eds.), Techniques for Characterization of Electrodes and Electrochemical Systems, J. Wiley, 1991, p. 581.
[15] F. Mansfeld, in: P. Marcus, F. Mansfeld (Eds.), Analytical Methods in Corrosion Science and Engineering, CRC Press, 2005 (ch. 13).
[16] F. Mansfeld, C.H. Tsai, H. Shih, ASTM STP 1154 (1992) 186.
[17] F. Mansfeld, H. Shih, H. Greene, C.H. Tsai, ASTM STP 1188 (1993) 37.
[18] F. Mansfeld, Corros. Sci. 47 (2005) 3178.